E&G Quaternary Sci. J., 74, 151–168, 2025
https://doi.org/10.5194/egqsj-74-151-2025

Open Access E&G Quaternary Science Journal

Research article

The Last Glacial Maximum (LGM) glacier network of the Valsugana area (south-eastern European Alps and Prealps, NE Italy)

Lukas Rettig[1], Sandro Rossato[2], Sarah Kamleitner[3,4], Paolo Mozzi[1], Susan Ivy-Ochs[4], Enrico Marcato[5], Marcus Christl[4], Silvana Martin[1], and Giovanni Monegato[2,6]

[1]Department of Geosciences, University of Padova, Padova, 35131, Italy
[2]National Research Council, Institute of Geosciences and Earth Resources, Padova, 35127, Italy
[3]Institute of Earth Surface Dynamics, University of Lausanne, Lausanne, 1015, Switzerland
[4]Laboratory of Ion Beam Physics, ETH Zurich, Zurich, 8093, Switzerland
[5]Studio Marcato, Vicenza, 36100, Italy
[6]Istituto Nazionale di Geofisica e Vulcanologia (INGV), Roma, Italy

Correspondence: Sarah Kamleitner (sarah.kamleitner@unil.ch) and Giovanni Monegato (giovanni.monegato@igg.cnr.it)

Relevant dates: Received: 26 February 2025 – Revised: 29 June 2025 – Accepted: 18 July 2025 – Published: 2 October 2025

How to cite: Rettig, L., Rossato, S., Kamleitner, S., Mozzi, P., Ivy-Ochs, S., Marcato, E., Christl, M., Martin, S., and Monegato, G.: The Last Glacial Maximum (LGM) glacier network of the Valsugana area (south-eastern European Alps and Prealps, NE Italy), E&G Quaternary Sci. J., 74, 151–168, https://doi.org/10.5194/egqsj-74-151-2025, 2025.

Abstract: We present new chronological and palaeoclimatological constraints on the evolution of the Valsugana glacier network (south-eastern European Alps) during the Last Glacial Maximum (LGM). The detection of ice-marginal sediments and landforms, related to the geological mapping of the area at 1 : 50 000 scale (CARG project, sheet 061 "Borgo Valsugana"), enabled a detailed reconstruction of past glaciers at their maximum extent. Chronological control on the geomorphological evidence is obtained using ^{10}Be surface exposure dating of erratic boulders from lateral moraine ridges at Monte Lefre, a nunatak within the LGM ice network. The exposure ages cluster between 20 and 19 ka, demonstrating that lateral moraines were formed at the very end of the LGM and that ice surface lowering in the area did not start prior to ca. 19 ka. Isolated from the Valsugana glacier network, several smaller ice masses developed. The reconstruction of four of these isolated glaciers and their equilibrium line altitudes (ELAs) allows us to better understand the climatic conditions that controlled glacier evolution during the LGM: glacier ELAs were lowest in the Venetian Prealps (ca. 1300–1500 m a.s.l.) and were gradually rising towards the more internal mountain chains (ca. 1500–1700 m a.s.l.). This ELA gradient suggests that precipitation sourced from the Mediterranean Sea was highest in the vicinity of the Alpine fringe, with successive moisture starvation towards the north. The detailed glacier reconstructions, the chronological data, and the palaeoclimatological insights may serve as ground control for future modelling efforts of large and interconnected palaeoglacier networks.

Published by Copernicus Publications on behalf of the Deutsche Quartärvereinigung (DEUQUA) e.V.

Kurzfassung: Wir präsentieren neue geochronologische und paläoklimatische Daten zur Entwicklung des glazialen Eisstromnetzes im Valsugana (südöstliche Europäische Alpen) während des Letzteiszeitlichen Maximums (LGM). Die Kartierung glazialer Sedimente und Landschaftsformen im Zuge der Erstellung der regionalen geologischen Grundlagenkarte (CARG-Projekt, Blatt 061 "Borgo Valsugana"), ermöglichte eine detaillierte Rekonstruktion der Gletscher zum Zeitpunkt ihrer größten Ausdehnung. Die chronologische Einordnung wurde mithilfe der ^{10}Be-Oberflächenexpositionsdatierung von erratischen Blöcken auf Seitenmoränen am Monte Lefre, einem Nunatak im Eisstromnetz, vorgenommen. Die Expositionsalter fallen größtenteils in den Zeitraum zwischen 20 und 19 ka, was zeigt, dass die Bildung dieser Seitenmoränen bis zum Ende des LGMs andauerte und dass die Absenkung der Eisoberfläche nicht vor ca. 19 ka begann. Mehrere kleinere Gletscher entwickelten sich unabhängig vom Valsugana-Eisstromnetz. Die Rekonstruktion vierer dieser isolierten Gletscher und ihrer Gleichgewichtslinien (ELAs) erlaubt ein besseres Verständnis der klimatischen Bedingungen, die die Entwicklung der LGM-Gletscher beeinflussten: ELAs waren am niedrigsten in den Venezianischen Voralpen (ca. 1300–1500 m) und stiegen allmählich in Richtung des inneralpinen Raums an (ca. 1500–1700 m). Dieser ELA-Gradient deutet darauf hin, dass der aus dem Mittelmeerraum stammende Niederschlag in der Nähe des Alpenrands am höchsten war und gegen Norden kontinuierlich abnahm. Die detaillierten Gletscherrekonstruktionen, die chronologischen Daten und die paläoklimatischen Erkenntnisse dieser Studie können zur Validierung künftiger Modellierungen großer und komplexer Eistromnetze hilfreich sein.

1 Introduction

Reconstructing the extent of Alpine glaciers during past glacial maxima has been attempted since the first palaeoglaciological studies (Penck, 1882; Penck and Brückner, 1901–1909). The attribution to the Würmian for the youngest glacial landforms and related deposits (Penck and Brückner, 1901–1909; Chaline and Jerz, 1984) enabled the reconstruction of the size and the limits of the Alpine glacier network at different scales, including the whole mountain chain (Castiglioni, 1940) or parts of it (Jäckli et al., 1973; van Husen, 1987). More recent maps (Ehlers and Gibbard, 2004; Bini et al., 2009; Coutterand et al., 2009; Ehlers et al., 2011) have shown an increased effort to depict details, aided by new surveys and enhanced chronological knowledge of key sites, especially within the end-moraine systems on both sides of the Alps (Monegato et al., 2007, 2017; Ivy-Ochs et al., 2018; Braakhekke et al., 2020; Kamleitner et al., 2022, 2023; Roattino et al., 2023; Pezzotta et al., 2024). In addition, glacier equilibrium line altitudes (ELAs) have been calculated for a few mountain groups along the fringe of the Alps (Monegato, 2012; Rettig et al., 2023) or generally reconstructed for the Alpine glacier network through modelling (Kuhlemann et al., 2008), providing constraints on the climatic conditions under which the Alpine glaciers evolved.

The internal parts of the glacier network, on the other hand, have been more challenging to study, partly because late-glacial and postglacial periglacial and gravitational processes have often obscured the evidence left by the glaciers during the Last Glacial Maximum (LGM, 26.5–19 ka according to Clark et al., 2009). Inner-alpine ice surface lowering has been chronologically constrained through surface exposure dating in the central and western parts of the Alps (Wirsig et al., 2016), but for the south-eastern Alps such chronological data supporting glacier reconstructions are still missing. Additionally, this sector of the Alps was characterized by the presence of small and isolated glaciers during the LGM. The study of these marginal glaciers has resulted in important palaeoclimate reconstructions for the area (Rettig et al., 2021, 2023). However, the evolution of these smaller ice masses in relation to the main glacier network has not been studied in detail yet.

The present work provides a detailed reconstruction of the LGM glaciers in the south-eastern Alps (Fig. 1a), including the Valsugana, which topographically corresponds to the upper trunk valley of the Brenta River catchment, and the Venetian Prealps. New exposure datings from a nunatak emerging from the Valsugana glacier network provide chronological constraints on regional glacier advance and retreat, while the ELA modelling of isolated glaciers, within and outside the limits of the glacier network, highlights the climatic gradient from the foreland plain to the inner sector of the Alps.

2 Setting

The south-easternmost sector of the Alps is characterized by a mountain belt, namely the Venetian Prealps, which separates the internal and highest parts of the southern Alps (i.e. the Dolomites) from the Venetian–Friulian Plain (Ivy-Ochs et al., 2022). The major catchments of this sector are (1) the Adige–Sarca, the largest catchment on the southern side of the Alps, (2) the Brenta, and (3) the Piave (Fig. 1a). The Venetian Prealps are characterized by carbonate plateaus (Antonelli et al., 1990; Barbieri and Grandesso, 2007),

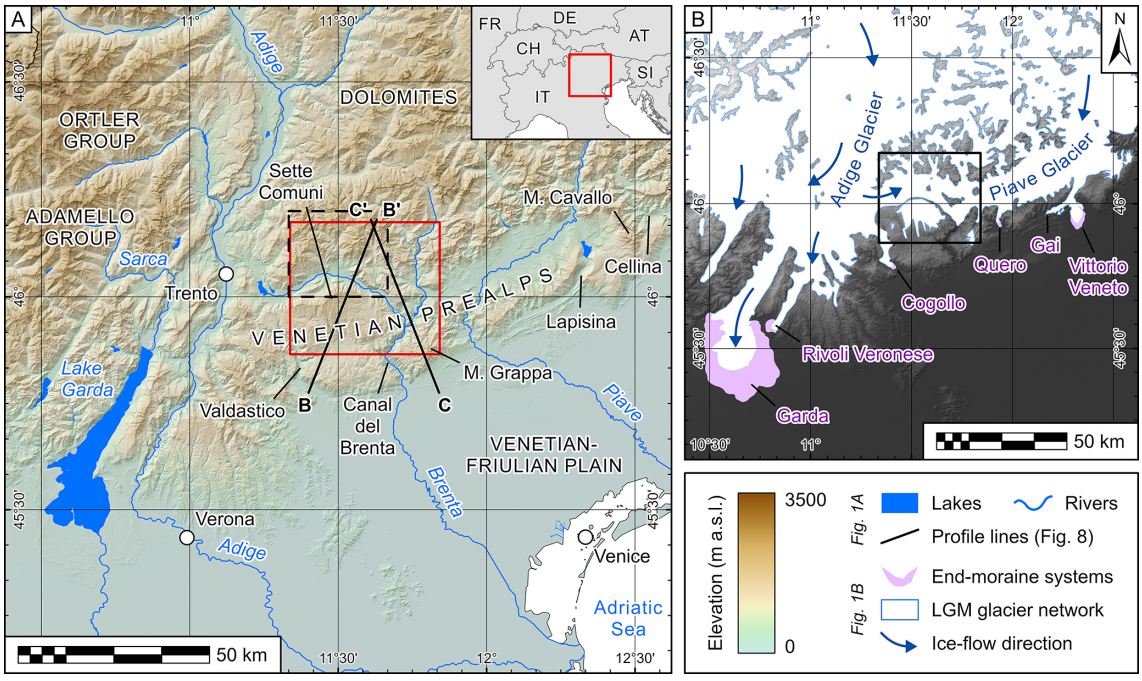

Figure 1. **(a)** Topographic map of the south-eastern Alps, depicting the major rivers draining the mountainous catchments. The study site (including the Valsugana) is marked by a red rectangle, corresponding to the extent of Fig. 2, and the profile lines refer to Fig. 8. The frame of the "Borgo Valsugana" sheet of the geological map is indicated with a dashed black line. **(b)** Reconstruction of the LGM glacier extent in the south-eastern Alps, modified from Ehlers et al. (2011), and the locations of the end-moraine systems related to the Adige–Sarca and Piave glaciers. Note the transfluence of ice from the Adige Valley towards the Valsugana. End-moraine systems were digitized following Monegato et al. (2017) and Carton et al. (2009). Elevation data: Copernicus DEM GLO-30 (access at https://dataspace.copernicus.eu/explore-data/data-collections/copernicus-contributing-missions/collections-description/COP-DEM, last access: 1 October 2025). Reference system for this map and all following map frames: WGS 1984.

whose elevation exceeds 1000 m a.s.l., reaching 2300 m a.s.l. at the northern rim of the Sette Comuni Plateau (Fig. 2). These plateaus are cut by only a few narrow canyons, namely Valdastico, Canal del Brenta (the Brenta River valley downstream of the Valsugana), Piave, Lapisina, and Cellina canyons/gorges (Fig. 1a). The Venetian Prealps are affected by tectonic uplift related to the activity of the thrust front of the eastern Southern Alps (e.g. Galadini et al., 2005; Poli et al., 2024). The Valsugana is also shaped by major tectonic structures, which led to a lower topography in respect to the neighbouring sectors, with the presence of mounts between 1400 and 1600 m a.s.l. and several wind gaps (see Fig. 2).

During the LGM, the principal valleys of the south-eastern Alps hosted a valley glacier network with the largest outlet glaciers (e.g. the Adige–Sarca or the Piave glaciers) spreading as piedmont lobes on the foreland plain (Ehlers and Gibbard, 2004; Ivy-Ochs et al., 2022). Despite the size of the mountain catchments, the piedmont plain in between the Garda and the Vittorio Veneto morainic amphitheatres is characterized by a lack of frontal moraines (Fig. 1b). The Venetian Prealps acted as a barrier to spreading valley glaciers and hosted local ice caps in the Sette Comuni Plateau, Monte Grappa, and Monte Cavallo during the LGM (Baratto et al., 2003; Cucato, 2007; Rettig et al., 2023). For these local/isolated glaciers in the Venetian Prealps, ELAs between 1320 and 1680 m a.s.l. were calculated with lower values (down to 1100 m a.s.l.) moving eastwards through the Carnic and to the Julian Prealps (Rettig et al., 2021, 2023). To the north, the valleys of the Dolomites were characterized by glacier networks. The large Adige glacier flowed into the Astico Valley, with the front at Cogollo (Fig. 1b; Cucato, 2001, 2007; Rossato et al., 2013), and into the Valsugana (Avanzini et al., 2010), where it merged with the Cismon–Piave glacier (Rossato et al., 2018). The Piave glacier flowed both into its modern valley, terminating at Quero (Venzo, 1977), and through the Lapisina Valley, forming the frontal moraines at Gai (Venzo, 1977) and at Vittorio Veneto (Fig. 1b; Bondesan et al., 2002; Carton et al., 2009).

3 Materials and methods

3.1 Geomorphological and sedimentological mapping

The geomorphological investigation of the area was performed through a combination of field surveys, related to the realization of the sheet 061 "Borgo Valsugana" of the geological map of Italy at 1 : 50 000 scale (Roghi et al., 2023), and

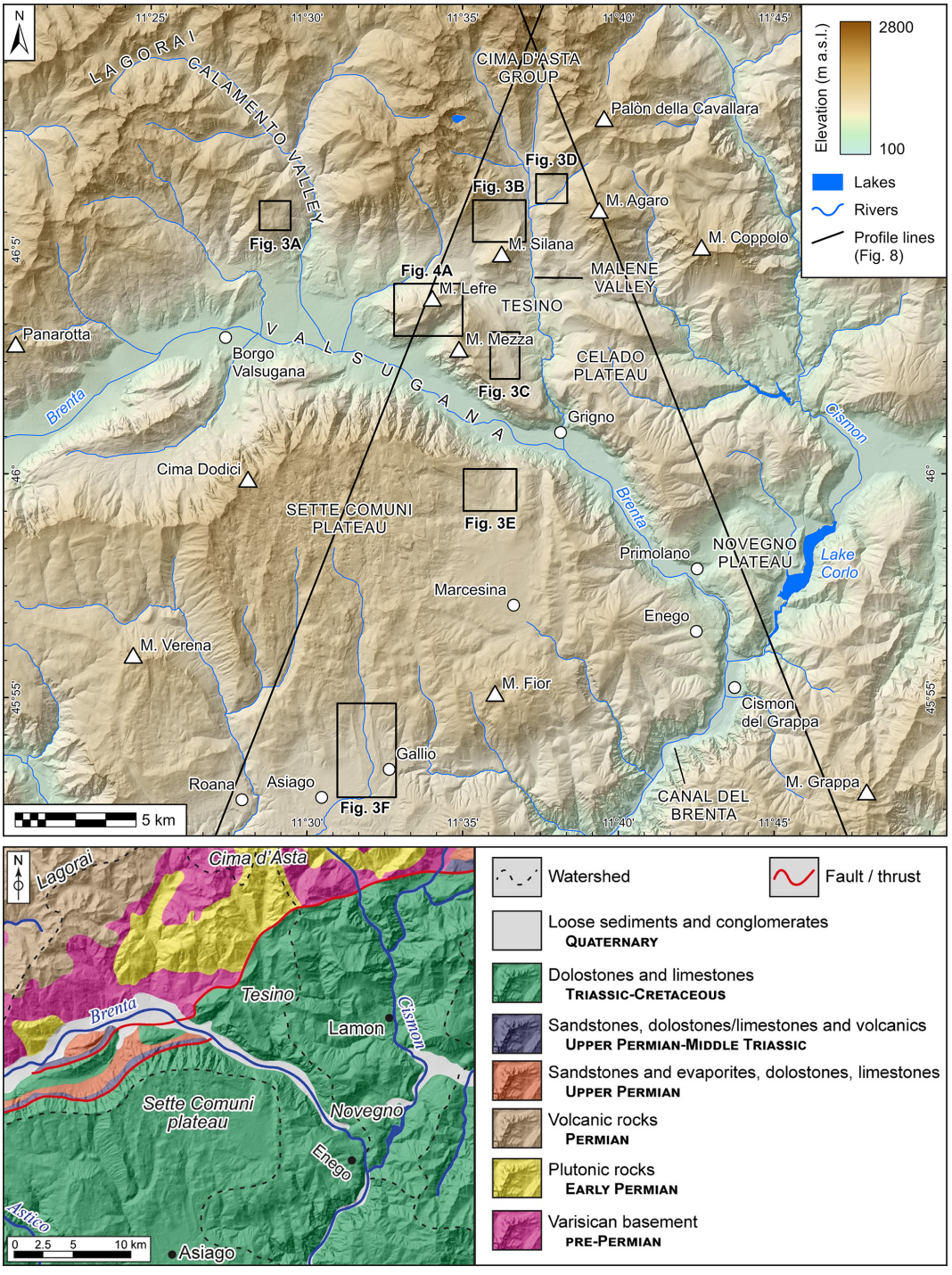

Figure 2. Topographic (upper panel) and geological (lower panel) map of the study site, the Valsugana sector of the south-eastern Alps; see Fig. 1 for its broader location. The west–east-trending trunk valley, through which the Brenta River flows, separates the carbonate Sette Comuni Plateau to the south from the Lagorai and the Cima d'Asta mountain groups to the north. The map extents of Fig. 3a–e (examples of glacial landforms) and Fig. 4a (Monte Lefre) are indicated by black rectangles. Black lines are the traces of profiles in Fig. 8. Elevation data: TINITALY DEM v.1.1 (Tarquini et al., 2007, 2023, access at https://tinitaly.pi.ingv.it, last access: 25 February 2025). Geological sketch map after Rossato et al. (2018).

mapping from remotely sensed datasets. The approach complies with present-day standards in geomorphological mapping of glaciated areas (Smith et al., 2006; Chandler et al., 2018). The remotely sensed data included both digital elevation models (DEMs) and orthophotos that were derived from the geoportals of Provincia Autonoma di Trento (https://siat.provincia.tn.it/stem, last access: 25 February 2025) and Regione Veneto (https://idt2.regione.veneto.it, last access: 25 February 2025) and integrated into a geographic information system (GIS) environment (Esri ArcGIS Pro v.3.2). Quaternary deposits were recognized and interpreted in the field based on their sedimentary properties, such as grain size, clast shape, lithology, or bedding structures (Evans and Benn, 2021). Special attention was paid to relative age indicators of the deposits, including their colours (via Munsell colour chart), the development of soils, and the degree of cementation (e.g. Burke and Birkeland, 1979; Colman and Pierce, 1986; Lukas, 2016). These properties were then compared to the location and elevation of the landforms where numerical age data were obtained (see next section). The suite of ice-marginal deposits, including erratic boulders, and landforms was used to constrain the limits of the palaeoglacier network and to create a new map of the LGM glaciation at the study site.

3.2 Surface exposure dating

Surface exposure dating using the terrestrial cosmogenic nuclide ^{10}Be (Gosse and Phillips, 2001; Ivy-Ochs and Kober, 2008) was applied to date the formation of lateral moraine ridges at Monte Lefre, a nunatak within the Valsugana glacier network (see Fig. 2 for the location of Monte Lefre). Four erratic boulders were selected and sampled after a careful evaluation of their size (ideally standing at least 1 m above surrounding ground), their position (at the centre of the moraine crest), and the preservation of boulder surfaces (no signs of chipping of the surface or of anthropogenic reworking; see Akçar et al., 2011). The moraines consist mainly of matrix-supported diamict, and therefore the possibility of post-depositional instabilities and exposure changes is given (Tomkins et al., 2021). However, by choosing boulders that were embedded in the matrix we aimed at avoiding those that had been moved after deposition. Two boulders (LEF-1 and LEF-2) are Permian rhyolites; the other two (LEF-3 and LEF-4) are granites. Approximately 1 kg of material was taken from each boulder by first sawing a rectangular grid into the rock surface with an angle grinder and then extracting cubes using hammer and chisel. The inclination of the sampled surfaces and azimuth/altitude values of the surrounding horizon were measured in the field using a compass clinometer and later refined through the PeakFinder web interface (https://www.peakfinder.com, last access: 25 February 2025). From these values a topographic shielding factor was calculated through the respective tool in the online calculators formerly known as the CRONUS-Earth calculators (Balco et al., 2008; https://hess.ess.washington.edu, last access: 25 February 2025).

The sampled material was crushed and sieved to a grain size between 800 and 250 µm using a Retsch BB 50 jaw crusher at the Department of Geosciences, University of Padova. Afterwards the samples were transferred to the Laboratory of Ion Beam Physics (LIP) at ETH Zürich, where they underwent chemical treatment following established protocols (Kohl and Nishiizumi, 1992; Ivy-Ochs, 1996; Kronig et al., 2018) to isolate quartz grains and to extract Be from the purified quartz. This involved leaching the samples in hydrochloric acid (HCl) and several times in weak (4 %) hydrofluoric (HF) acids so that feldspar grains were progressively dissolved. Magnetic minerals were removed using a Frantz model L-1 isodynamic separator. The purified quartz was then spiked with ca. 250 µg of a ^{9}Be carrier in solution (Scharlau, 1000 ppm) and dissolved in concentrated (40 %) HF. Two sets of ion exchange columns were used to clean the dissolved samples and remove unwanted cations and anions. Subsequent addition of ammonia solution induced the pH-selective precipitation of beryllium hydroxide ($Be(OH)_2$), which was then ignited to beryllium oxide (BeO), the target compound for accelerator mass spectrometry (AMS) measurements.

The AMS measurements of ^{10}Be concentrations were carried out using the 0.3 MV MILEA system at LIP (Maxeiner et al., 2019). The concentrations were normalized against an internal standard (S2007N) with a ^{10}Be / ^{9}Be ratio of 28.1×10^{-12} and corrected for a full process blank of $(3.18 \pm 1.26) \times 10^{-15}$. The CRONUS-Earth calculators (Balco et al., 2008) were used to calculate exposure ages from the ^{10}Be concentrations. The ages in this paper are reported both with internal 1σ errors, related to uncertainties in the AMS measurement only, and with external 1σ errors in brackets, the latter also including uncertainties within the applied ^{10}Be production rate. They were calculated with the ^{10}Be production rate based on the Northeastern North America (NENA) calibration dataset (Balco et al., 2009) and the scaling scheme for spallation of Lal (1991) and Stone (2000). The NENA production rate is consistent with a regional production rate determined by Claude et al. (2014) at the Chironico landslide in southern Switzerland. Differences in calculated age between the two are less than 2 %. NENA is used to allow straightforward comparison to ^{10}Be ages from other Alpine sites (Ivy-Ochs et al., 2018; Kamleitner et al., 2022). In the absence of quantitative estimates for surface denudation rates of the sampled rock types, a value of 1 mm ka^{-1} was applied to account for limited surface erosion of the generally very resistant lithologies (André, 2002). The erosion correction increased the exposure ages by 0.6 %–1.6 % compared to the zero-erosion values, which is well within the respective uncertainty range of the method (see Table 1). No correction for shielding by snow cover was applied because the height of the boulders above the ground (at least 80 cm; see Table 1) usually exceeds the thickness of the snowpack in the region:

at the meteorological station in Asiago (1000 m a.s.l.), a snow thickness of 80 cm was reached on average only on five days a year during the period between 1961 and 1990 (Valt et al., 2022).

3.3 Palaeoglacier, ELA, and palaeoprecipitation reconstructions

A reconstruction of four smaller and isolated ice masses in the study area was carried out to obtain estimates of local ELAs and ultimately to better constrain the climatic conditions under which the LGM glaciers in the Valsugana evolved. The reconstructions are based not only on the mapped geomorphological evidence, in particular on the locations of frontal and lateral moraine ridges, but also on trimlines and lateral meltwater channels. These "target features" were first digitized within ArcGIS Pro and then used to constrain the semi-automated toolbox PalaeoIce (Li, 2023). This toolbox represents an implementation of the standard flow law of ice and produces a three-dimensional glacier surface by assuming perfectly plastic ice rheology (Nye, 1952, 1965; Schilling and Hollin, 1981; Benn and Hulton, 2010). It works similarly to the more widely used toolbox GLARE (Pellitero et al., 2016), but the user can automatically constrain the reconstruction to lateral target features so that the output glacier surface is in line with the morphological evidence. Once a satisfactory glacier surface had been reconstructed, ELAs were calculated using both the accumulation area ratio (AAR) and the area–altitude balance ratio (AABR) methods (Furbish and Andrews, 1984; Rea, 2009; Pellitero et al., 2015). For both approaches, global median values as determined by Oien et al. (2022) – an AABR of 1.56 and an AAR of 0.58 – were selected.

To discuss the palaeoclimatic significance of the reconstructed ELAs, a calculation of palaeoprecipitation was attempted for the four isolated glaciers, based on the quantitative relationship between summer (June, July, August) air temperature and annual precipitation at the ELA (Ohmura and Boettcher, 2018). This was achieved by the following methodological steps: (1) retrieving present-day (1971–2000) average summer (June, July, August) temperatures from the HISTALP dataset by Auer et al. (2007), (2) correcting for an altitudinal temperature lapse rate of 0.0065 °C m^{-1}, (3) assuming a summer temperature drop of ca. 10 °C during the LGM, as suggested by pollen (Pini et al., 2022) and chironomid data (Samartin et al., 2016) as well as palaeoclimate models (Del Gobbo et al., 2023), and (4) using the P/T relationship at the ELA presented in Ohmura and Boettcher (2018). We acknowledge that there are considerable uncertainties related to absolute values of palaeoprecipitation calculated from ELAs (cf. Rettig et al., 2023; Hofmann et al., 2024) and therefore discuss only the relative differences between the sites to identify spatial gradients within palaeoprecipitation.

4 Results

4.1 Geomorphological and geological evidence

The lateral and terminal moraines, pertaining both to isolated glaciers and to the valley glacier network, are important geomorphological and sedimentary features, indicating the location and the elevation of the ice surface (see Fig. 3 for examples of these moraines). Moraines in the Valsugana are made of matrix-supported diamicton, with a sandy–silty matrix. Clasts are subrounded to subangular, and the deposits are normally consolidated. The thickness is variable from some metres to tens of metres. Lateral moraines related to the Valsugana trunk glacier are preserved in flat sectors of the valley slopes at elevations ranging from 1550 m a.s.l. in the Panarotta area to around 1500 m a.s.l. at the outlet of Calamento Valley (Fig. 3a). A key area is the Monte Lefre (Fig. 4a), a limestone massif encircled by smoothed moraines at about 1360 m a.s.l. Here, several erratic boulders are scattered, four of which were sampled for exposure dating (Fig. 4b–e). The topmost part of the mountain, on the other hand, shows intensely weathered diamicton (Munsell colour 5YR) and diamictite made of subrounded clasts and boulders of crystalline and rhyolite rocks, while carbonates are lacking or strongly altered (Fig. 5). To the north, the glacial deposits crop out at a similar elevation, forming distinguishable moraines in the saddle between Monte Silana and Monte Fierollo (Fig. 3b). The abundance of rhyolite blocks in these deposits is remarkable because this rock type does not crop out in the Cima d'Asta massif. On the left side of the Malene Valley, the moraines marking the glacier limits dammed the Rio Secco Valley (Fig. 3d) and are also located south of La Rocchetta (1240 m a.s.l.) and at Prati di Monte Mezza (Fig. 3c; 1230 m a.s.l.). In the Celado Plateau (see Fig. 6), the bedrock is present at higher elevation than at the Tesino, and only across a saddle at 1666 m a.s.l. were scattered exotic rounded pebbles found. To the south, the lateral moraines of Enego (around 800 m a.s.l.) are close to the frontal position of the Valsugana glacier (Rossato et al., 2018). To the east, the Novegno Plateau (Fig. 6) hosts radial morainic ridges at about 710 m a.s.l. with a related left moraine at the other side of the wind gap located between the Celado and Novegno plateaus (Fig. 3g; Rossato et al., 2018). The south-eastern sector of the study area, along the north-western slope of Monte Grappa, is marked by moraines related to the Cismon–Piave glaciers. Ridges are located at about 750 m a.s.l. (Rossato et al., 2018), whereas deeply weathered glacial deposits were found up to 900 m a.s.l. The Piave glacier also formed the moraines that dammed the Seren Valley.

The Sette Comuni ice cap created several frontal moraines at the outlets of the major valleys: at Roana and Gallio to the south and at Marcesina to the east (Fig. 3f). Lateral moraines are also present towards the northern rim at the Barricata gap

Table 1. Details on the erratic boulders that were sampled for surface exposure dating, ^{10}Be concentrations determined via AMS, and exposure ages with internal and external (in brackets) errors assuming 0 and 1 mm ka^{-1} erosion rates.

	Boulder size ($L \times W \times H$)	Coordinates (WGS 1984)		Elevation	Sample thickness	Topographic shielding	^{10}Be concentration	Exposure age 1 mm ka^{-1}	Exposure age 0 mm ka^{-1}
	[m]	[° N]	[° E]	[m a.s.l.]	[cm]	factor	[$\times 10^5$ at g^{-1}]	erosion [ka]	erosion [ka]
LEF-1	$3.0 \times 2.0 \times 0.8$	46.0634	11.5749	1346	1.2	0.9987	2.355 ± 0.053	19.6 ± 0.5 (1.1)	19.3 ± 0.4 (1.0)
LEF-2	$3.0 \times 1.5 \times 1.5$	46.0634	11.5751	1341	1.6	0.9969	0.822 ± 0.028	6.8 ± 0.2 (0.4)	6.8 ± 0.2 (0.4)
LEF-3	$2.5 \times 1.7 \times 1.2$	46.0617	11.5565	1340	1.2	0.9995	2.314 ± 0.062	19.4 ± 0.5 (1.1)	19.1 ± 0.5 (1.1)
LEF-4	$8.0 \times 4.5 \times 3.5$	46.0615	11.5560	1332	1.5	0.9995	2.205 ± 0.086	18.6 ± 0.7 (1.2)	18.3 ± 0.7 (1.1)

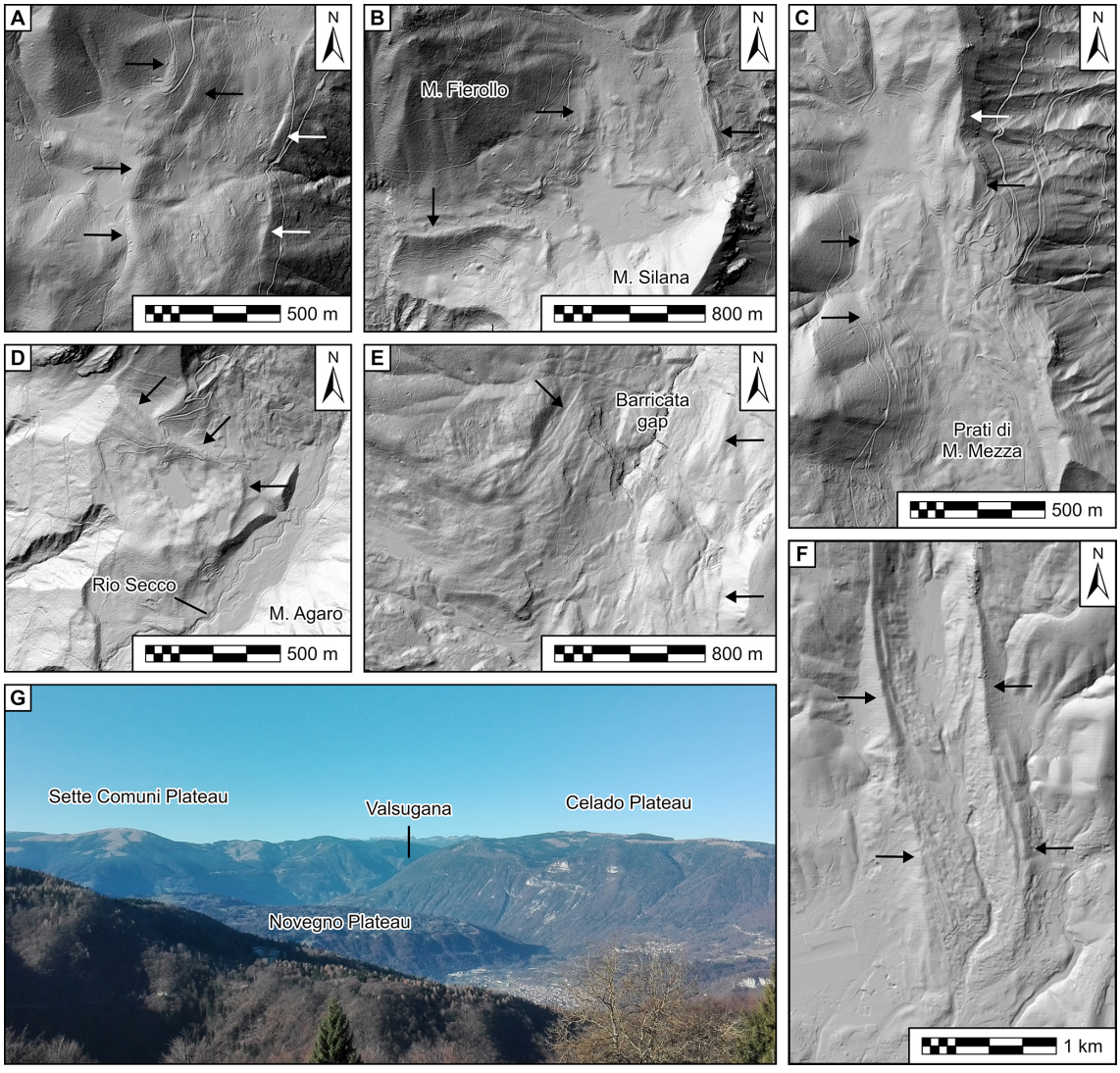

Figure 3. Examples of ice-marginal landforms used for reconstructing the extent of the Valsugana glacier network. **(a)** Lateral moraines at the outlet of the Calamento Valley. **(b)** Moraines in the saddle between Monte Silana and Monte Fierollo. **(c)** Lateral moraines of Prati di Monte Mezza. **(d)** Left lateral moraine in the Malene Valley damming the Rio Secco tributary valley. **(e)** Lateral moraines at the Barricata gap at the confluence of the Sette Comuni ice cap with the trunk glacier in the Valsugana. **(f)** The frontal moraines at Gallio, related to an outlet glacier of the Sette Comuni ice cap. **(g)** View towards the Novegno Plateau and the lower part of the Valsugana. Elevation data in all panels: LiDAR PAT 2014 DEM (Provincia Autonoma di Trento, access at https://siat.provincia.tn.it/stem, last access: 25 February 2025) and DTM5 (Regione del Veneto, access at https://idt2.regione.veneto.it, last access: 25 February 2025). For the location of the landforms, see the topographic map (Fig. 2).

(Fig. 3e); their elevation (ca. 1200 m a.s.l.) is consistent with those on the left side of the Valsugana.

Other frontal moraines are located in areas within the glacier network but at higher elevation – these are related to isolated glaciers. Moraines at the southern side of Palòn della Cavallara (ca. 1550 m a.s.l.) are characterized by the abundance of rounded granite boulders and subrounded crystalline and carbonate clasts; their weathering is comparable to that of Monte Lefre. On the northern and eastern side of the Monte Agaro plateau, three moraines are located at elevation between 1520 and 1400 m a.s.l. The northern slopes of Monte Coppolo are characterized by frontal moraines at 1220 m a.s.l. and some remarkable lateral moraines damming small valleys to the left at 1525 and 1450 m a.s.l. A similar occurrence is related to the moraines located along the valleys of the Monte Grappa (Carraro and Sauro, 1979; Baratto et al., 2003) and Monte Fior (Cucato, 2007) in the Prealps south of the major valley glaciers.

4.2 Surface exposure ages

The four erratic boulders that were sampled for ^{10}Be surface exposure dating at Monte Lefre originate from two different lateral moraine ridges – at Malga Valle (LEF-1 and LEF-2) and about 1.5 km further to the west, close to the Chiesetta Alpina (LEF-3 and LEF-4; see Figs. 4a and 5). Both moraines are located at very similar elevations (ca. 1340 m a.s.l.), suggesting that they represent the same ice-marginal position. The calculated exposure ages from all four boulders can therefore be regarded as a single dataset. Corrected for a surface erosion of 1 mm ka^{-1}, boulder ages (with external uncertainties) are 19.6 ± 1.1 ka (LEF-1), 6.8 ± 0.4 ka (LEF-2), 19.4 ± 1.1 ka (LEF-3), and 18.6 ± 1.2 ka (LEF-4; see Table 1 and Fig. 4). Three out of the four ages have overlapping 1σ uncertainties and are tightly clustered around a best Gaussian fit of 19.3 ± 1.3 ka (the best Gaussian fit was calculated using the MATLAB/Octave code by Rodés, 2020). Only LEF-2 represents a clear outlier, suggesting that this boulder experienced some form of either post-depositional shielding, reworking, or movement, resulting in a much younger exposure age.

4.3 Reconstructions of isolated glaciers and their equilibrium line altitudes

In the study area, four glaciers that remained isolated from the Valsugana glacier network were reconstructed (see Fig. 6 for the location of the glaciers and Table 2 for detailed properties). The Monte Coppolo glacier (Fig. 7a) was the largest of the four reconstructed glaciers, with a surface area of ca. 4.4 km^2 and an estimated ice volume of 0.16 km^3. The glacier originated from two north-facing cirques at around 2000 m a.s.l., from which the ice was initially flowing towards the north and then bending slightly towards the east, where the frontal tongue reached a minimum altitude of ca. 1100 m a.s.l. On its western side the ice blocked the drainage of two small tributary valleys, which led to the deposition of fine-grained sediments in these valley bottoms. Both the AABR method and the AAR method yielded very similar ELAs of the Monte Coppolo glacier of 1540 and 1530 m a.s.l., respectively.

Approximately 5 km west of the Monte Coppolo, Monte Agaro (2062 m a.s.l.) hosted another isolated glacier of slightly smaller surface area (2.5 km^2) and ice volume (0.10 km^3, Fig. 7b). In its lower part, the Monte Agaro glacier split into three different tongues that descended into the valleys to the north and east of the massif. Frontal moraine ridges in these valleys indicate that the glacier front reached elevations between 1300 and 1500 m a.s.l. The ELA of the Monte Agaro glacier was calculated to 1740 m a.s.l. via the AABR method and to 1780 m a.s.l. via the AAR method.

Just to the north of the Monte Agaro, a glacier developed on the southern slope of the Palón della Cavallara (2199 m a.s.l., Fig. 7c). The south-facing Cavallara glacier was much smaller (surface area ca. 1.0 km^2, ice volume ca. 0.03 km^3) than the Monte Coppolo and Monte Agaro glaciers, but its ELA is comparable to the latter (1750 m a.s.l. via the AABR method, 1730 m a.s.l. via the AAR method).

The Monte Fior glacier (Fig. 7d, surface area ca. 2.2 km^2, ice volume ca. 0.13 km^3) was located on the western side of the Sette Comuni Plateau, around 20 km south of the previous three glaciers. From Monte Fior (1824 m a.s.l.) the glacier first flowed towards the north-east and then bent towards the south-east, following the course of the valley down to an elevation of ca. 1250 m a.s.l., where frontal moraine ridges are preserved. It is likely that ice also existed on the other flanks of Monte Fior; however no morphological or sedimentological evidence was found to reliably reconstruct the glacier extent in these sectors. The ELA of the Monte Fior glacier was calculated to 1660 m a.s.l. via the AABR method and to 1720 m a.s.l. via the AAR method.

5 Discussion

5.1 A new map of the LGM glaciers of the south-eastern Alps

The integrated geomorphological and chronological dataset allowed us to reconstruct the glacier network in the Valsugana (south-eastern Alps) during the LGM (Fig. 6). The major trunk glacier along the Valsugana was fed by the transfluence of a branch of the Adige glacier towards the east (see Fig. 1b). The ice surface of this glacier was at 1530 m a.s.l. south of Panarotta and had a very low gradient to the east, where it reached 1360 m a.s.l. at the Monte Lefre, ca. 17.5 km downvalley. In the sector of the trunk valley south of Monte Mezza, the glacier surface lowered to about 1200 m a.s.l. and merged with an outlet of the Sette Comuni ice cap closely upstream of Grigno (Fig. 6). A branch of the Valsugana glacier passed Monte Lefre and Monte Silana to the north and flowed

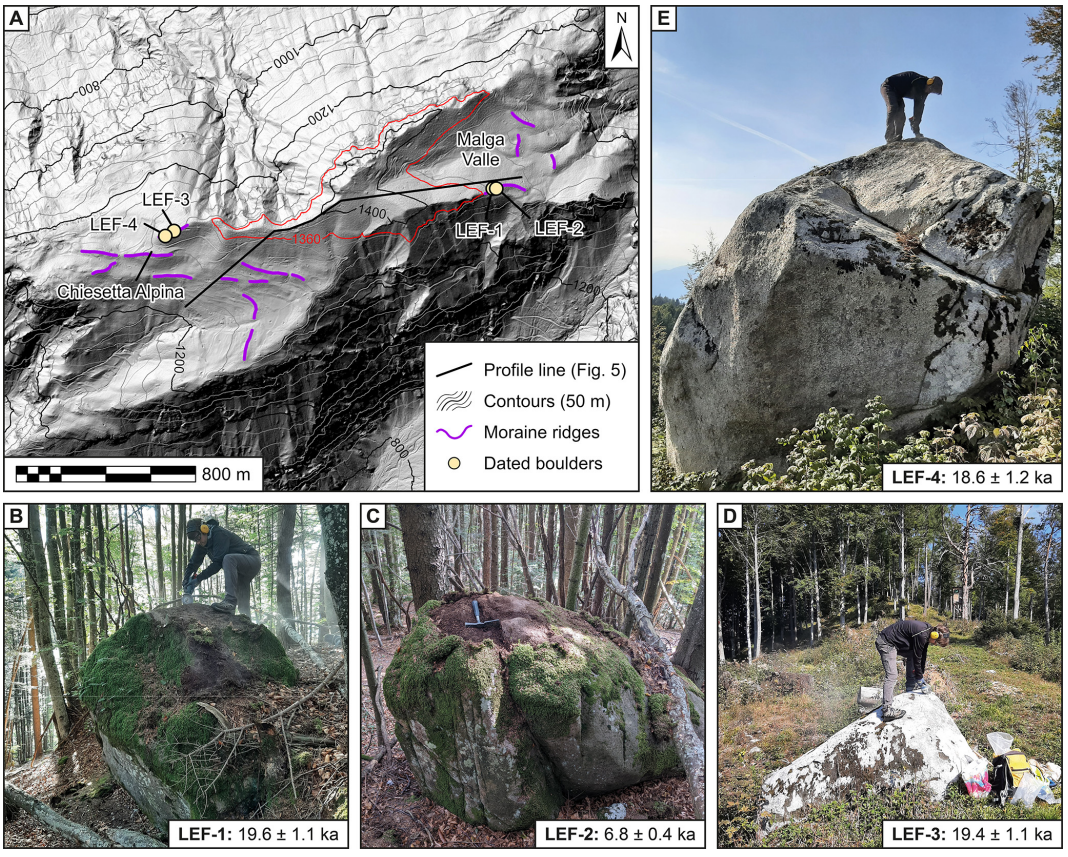

Figure 4. **(a)** Map of lateral moraine ridges at the Monte Lefre nunatak, with the locations of erratic boulders selected for ^{10}Be surface exposure dating. The red contour line (1360 m a.s.l.) indicates the approximate maximum elevation of the ice surface during the LGM. Elevation data: LiDAR PAT 2014 DEM (Provincia Autonoma di Trento, access at https://siat.provincia.tn.it/stem, last access: 25 February 2025). **(b–e)** Photographs of the boulders LEF-1, LEF-2, LEF-3, and LEF-4, visualizing how and where the samples for exposure dating were taken.

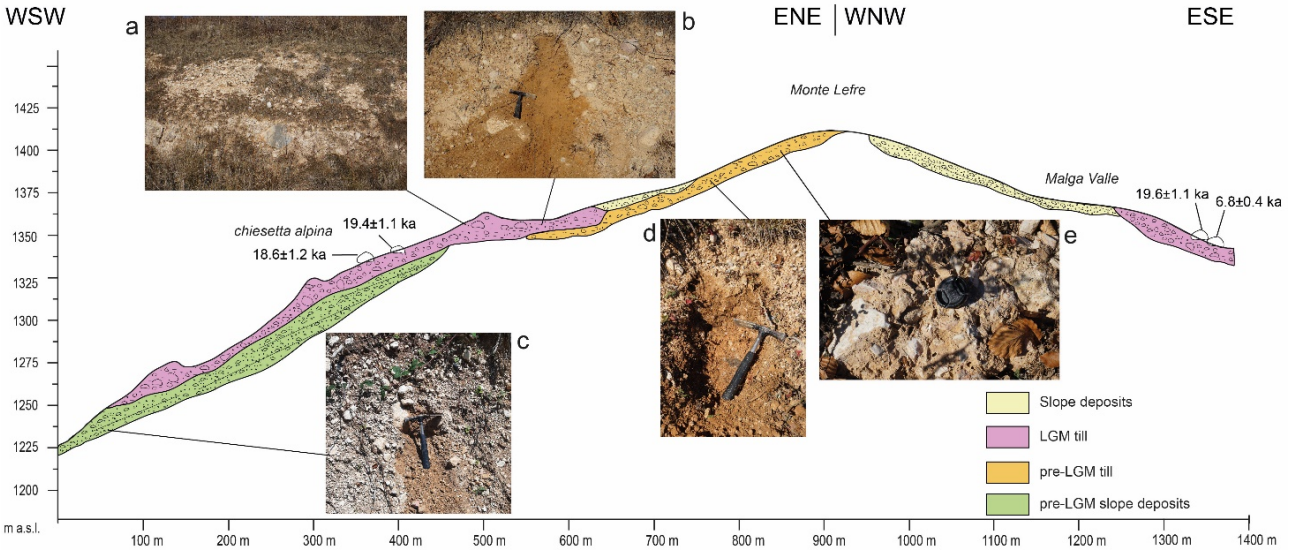

Figure 5. Cross section of the Monte Lefre showing the different stratigraphic units and the location of the dated boulders. The photos show from top left to bottom right **(a)** till associated with the dated boulders and **(b)** soil cover of the till, **(c)** carbonate slope deposits covered by LGM till, **(d)** well-developed soil at the top of the pre-LGM till, and **(e)** cemented till (pre-LGM).

Table 2. Key properties of the four reconstructed isolated LGM glaciers in the Valsugana including their ELAs, calculated via the AABR and the AAR methods. Map views of the glaciers are in Figs. 6 and 7.

	Lat [° N]	Long [° E]	Catchment aspect	Elevation range [m a.s.l.]	Flowline length [km]	Surface area [km^2]	Ice volume (km^3)	ELA (AABR 1.56) [m a.s.l.]	ELA (AAR 0.58) [m a.s.l.]
Monte Coppolo glacier	46.09	11.72	North	1070–1930	3.7	4.35	0.16	1540	1530
Monte Agaro glacier	46.10	11.66	North-east	1300–2060	3.1	2.49	0.10	1740	1780
Cavallara glacier	46.12	11.66	South-west	1450–2110	2.0	1.02	0.03	1750	1730
Monte Fior glacier	45.92	11.62	East	1250–1850	3.6	2.15	0.13	1660	1720

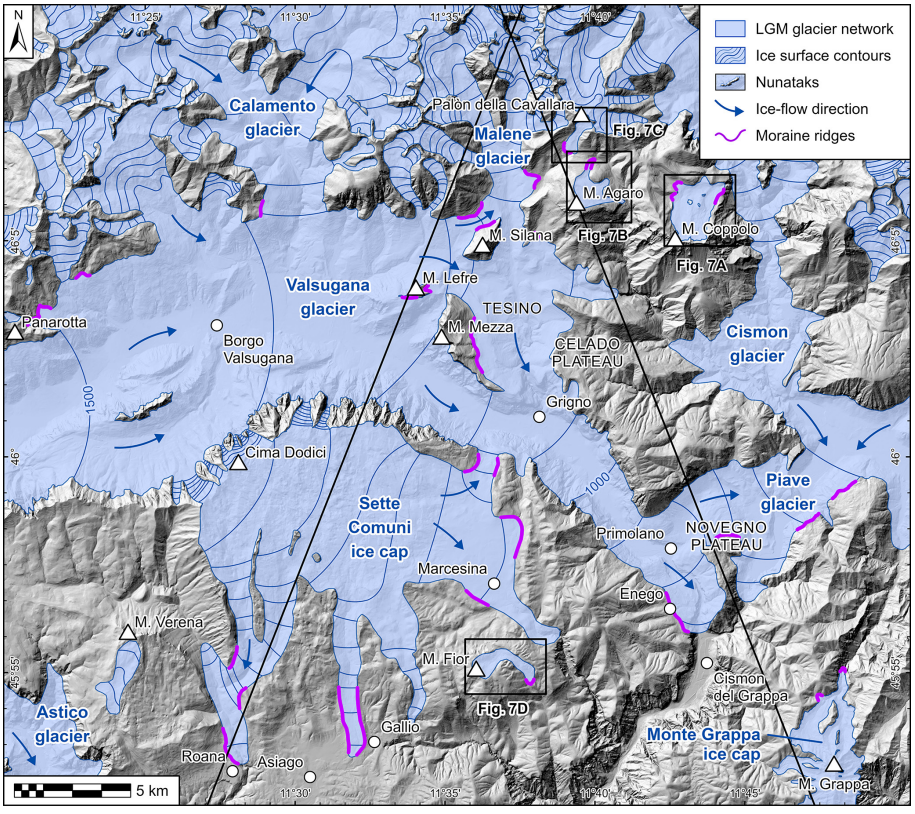

Figure 6. Reconstruction of the Valsugana glacier network (glaciers are labelled in blue) during the LGM, based on the results of geological and geomorphological mapping. Note the nunataks, such as Monte Lefre (Fig. 4a), that remained ice-free and the locations of smaller, isolated mountain glaciers (Fig. 7a–d) for which ELAs were reconstructed. Black lines are the traces of profiles in Fig. 8. Elevation data: TINITALY DEM v.1.1 (Tarquini et al., 2007, 2023, access at https://tinitaly.pi.ingv.it, last access: 25 February 2025).

into the Malene Valley, as testified by the abundance of rhyolite boulders and pebbles in the glacial deposits of the lower reach of the Malene Valley. The elevation of the glacier surface is marked here by several lateral moraines, which also dammed the Rio Secco Valley at 1315 m a.s.l. (cf. Fig. 3d) and the area at the south-western slope of Monte Agaro. From the Tesino sector, a branch of the glacier flowed eastwards but did not reach the Cismon trunk glacier, while most of the ice flowed to the south, leaving lateral moraines along the eastern slopes of Monte Mezza at 1220 m a.s.l. To the east of the glacier, the ice surface elevation was not sufficiently high for overflowing the Celado Plateau; here only glaciofluvial spillways formed. Moving south, this branch of the glacier merged again into the Valsugana trunk glacier at Grigno. Downstream of Grigno, the ice surface decreased from 1220 m a.s.l. to about 750 m a.s.l. at the frontal sector near Enego.

Considering the depth of the post-LGM valley fill in the upper Valsugana (Felber et al., 1998), an ice thickness of up to 1000 m can be estimated for the trunk glacier, which upon reaching Primolano had a width of about 600 m. Here the glacier was blocked by the narrowing of the Valsugana

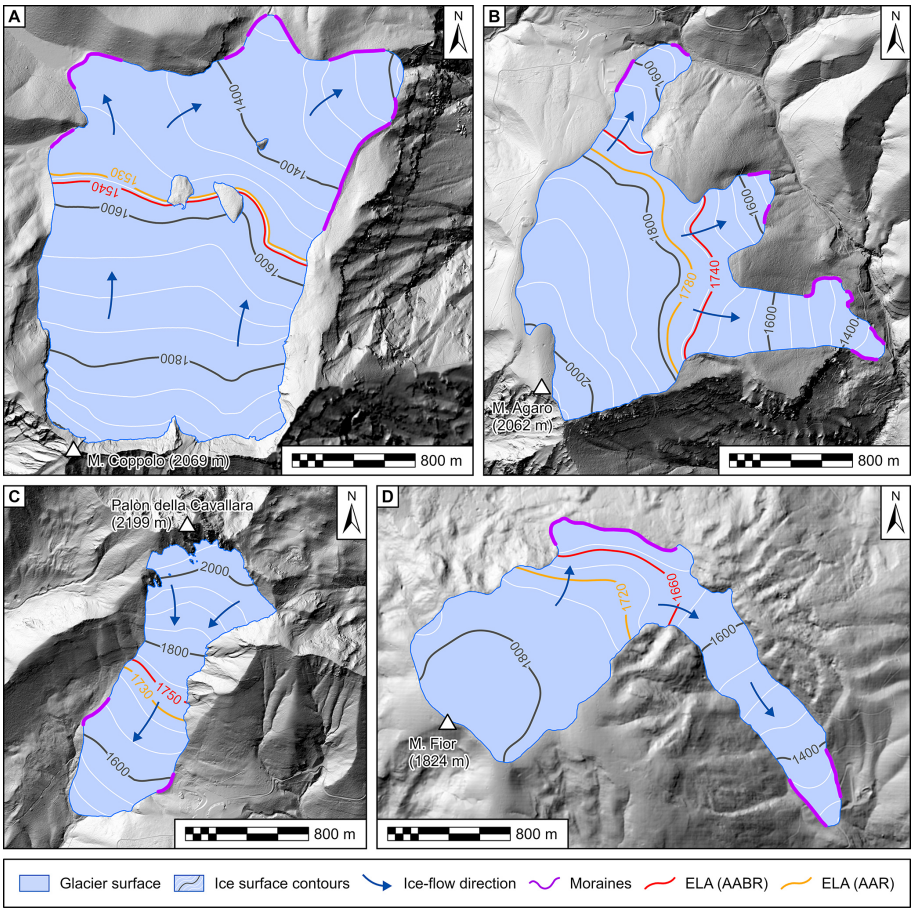

Figure 7. Reconstructions of isolated mountain glaciers and their ELAs. **(a)** The Monte Coppolo glacier. **(b)** The Monte Agaro glacier. **(c)** The Palòn della Cavallara glacier. **(d)** The Monte Fior glacier. All glacier ELAs were calculated using an AABR of 1.56 and an AAR of 0.58 (Oien et al., 2022). Elevation data for all panels: LiDAR PAT 2014 DEM (Provincia Autonoma di Trento, access at https://siat.provincia.tn.it/stem, last access: 25 February 2025) and DTM5 (Regione del Veneto, access at https://idt2.regione.veneto.it, last access: 25 February 2025).

Valley (at present the valley is less than 100 m wide) and was forced to cross the obstacle of the Novegno and Enego plateaus at 800 m a.s.l. The glacier split into two branches (Rossato et al., 2018), one climbing the plateau and crevassing downstream of the gorge and the other flowing to the east across a wind gap, at the end of which it merged with the Cismon–Piave glacier arriving from the north-east (Fig. 6). The Cismon trunk glacier merged with the westernmost branch of the Piave glacier 3 km upstream of the confluence with the Valsugana glacier; the resulting glacier front crevassed downstream of the Corlo Gorge, 60 m wide, now submerged by Lake Corlo (Fig. 2). The hypothesis of glacier crevasse cascades in this area is established by the lack of frontal moraines or glacial deposits in both the narrow valleys, whereas a 30 m thick glaciofluvial succession starts at this point (Rossato et al., 2018).

5.2 Timing of LGM glacier advances and moraine formation

The ^{10}Be surface exposure ages from erratic boulders at Monte Lefre chronologically constrain the mapped landform evidence and the reconstruction of the Valsugana glacier network described in the previous section. The data strongly point to a stabilization of the lateral moraine between 20 and 19 ka, as the best Gaussian fit of the ages (19.3 ± 1.3 ka), the oldest age (19.6 ± 1.1 ka), and the age of the largest boulder (18.6 ± 1.2 ka) are within this time bracket. The lateral moraines at Monte Lefre are located at elevations between ca. 1340 and 1360 m a.s.l. This coincides with the elevations of ice-marginal features in other parts of the valley, indicating that the glacier surface had been persistent at this elevation until ca. 19 ka. The lack of fresh (LGM) glacial deposits at higher elevations (cf. Fig. 5) suggests that those moraines also mark the maximum ice extent during the last glacial cycle. This is slightly at odds with data from moraine

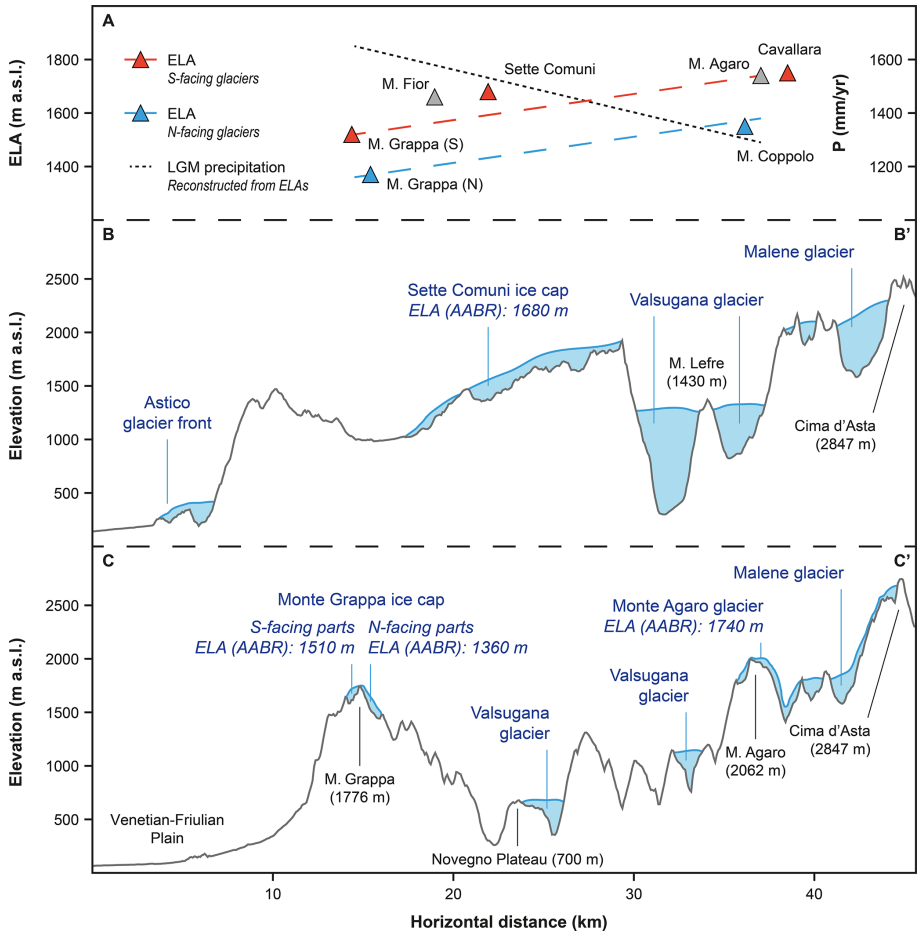

Figure 8. **(a)** ELA gradients from the Venetian–Friulian Plain to the study area with reconstructed glacier ELAs visualized as red (S-facing), blue (N-facing), and grey (E–W-facing) triangles; palaeoprecipitation values based on ELAs and palaeotemperature reconstructions (see "Materials and methods" section) are also presented. **(b)** Cross section from the Astico Valley to Cima d'Asta, crossing the Sette Comuni Plateau (Rettig et al., 2023) and Monte Lefre. **(c)** Cross section from the Venetian–Friulian Plain over the Monte Grappa (Baratto et al., 2003; Rettig et al., 2023) and the Monte Agaro towards Cima d'Asta. For the location of the profiles, see Fig. 1a.

amphitheatres along the south-eastern Alpine fringe. There, the maximum ice extent is usually recorded much earlier at around 26 to 24 ka, while the late LGM is connected to recessional moraines at more internal positions (Monegato et al., 2007, 2017). Also, the maximum aggradation within the alluvial fans in the Venetian–Friulian Plain was reached earlier: in the Brenta megafan, fed by outwash from the Valsugana glacier network, aggradation peaked between ca. 26.7 and 23.8 ka cal BP and subsequently decreased towards the latest part of the LGM (Rossato and Mozzi, 2016).

This temporal discrepancy may be due to different factors. End-moraine systems in the south-eastern Alps and alluvial fan aggradation are chronologically constrained by ^{14}C ages which are usually taken from the middle or the bottom of glacial sediment successions and therefore constrain the onset of sediment deposition. Exposure ages, on the other hand, are taken from the top of glacial landforms and therefore date the last depositional event. Another explanation might be that the ice surface in the inner parts of the glacier network remained relatively stable throughout the LGM, while climatic fluctuation mainly manifested in changes within the glacier front in the piedmont plain. Our data show that glaciers in the south-eastern Alps were still at an advanced position before ca. 19 ka. This provides important constraints for the initiation of ice surface lowering in the south-eastern Alps that compare to exposure ages from the central and western parts of the Alps, which indicate a lowering of the glacier surface after 18.5 ka (Wirsig et al., 2016). The onset of post-LGM deglaciation and ice retreat can therefore be bracketed in the intervening time period.

5.3 The equilibrium line altitude in the south-eastern Alps during the LGM

Above the trimline, but within the limits of the Valsugana glacier network, isolated glaciers developed in some mountains such as the Monte Agaro, Palòn della Cavallara, and

Monte Coppolo. Even if no chronological data are available for these sites, the degree of weathering and soil formation on top of the deposits is similar to that for deposits located in the Valsugana area and suggests a coeval formation of the isolated glaciers with the Valsugana glacier network. The ELA values calculated for the four isolated glaciers vary distinctly based on their different topographies and aspects; the lowest ELA (1540 m a.s.l.) was reconstructed for the Monte Coppolo glacier, with 4.4 km^2 being the biggest of the studied local glaciers. It is remarkable that this ELA is similar to the elevations of the highest lateral moraines of the Valsugana glacier and its major tributaries. It suggests that the ELA of the major glaciers in the area was likely comparable to that of the smaller ice masses, with accumulation areas widespread above 1540 m a.s.l. The Monte Agaro and Palón della Cavallara glaciers are located in the same sector; the first was a plateau glacier, 2.49 km^2 wide, that flowed towards N and E, and the second was a small (ca. 1 km^2) cirque glacier facing S. The similar ELAs of these glaciers (1740 and 1750 m a.s.l., respectively) are ca. 200 m higher than the ELA of the nearby Monte Coppolo glacier. This difference can probably be ascribed to the higher amount of solar radiation these glaciers received due to their aspect and/or lower steepness that enhanced ablation (Coleman et al., 2009). In the prealpine plateau sector, the large Sette Comuni ice cap had its accumulation area above 1680 m a.s.l. (Rettig et al., 2023). This glacier fed several lobes, one merging with the Valsugana glacier to the north and the others forming snouts to the south, filling narrow valleys. The Monte Fior glacier originated from a mountain of the plateau outside the flux of the main glacier. This small glacier (2.15 km^2) flowed to the east in a narrow valley. The calculated ELA is 1660 m a.s.l., very similar to that of the Sette Comuni ice cap (Rettig et al., 2023).

5.4 Climate gradient across the south-eastern Alps

Recently published palaeoclimate models show how atmospheric circulation affected the Alps during the LGM (Ludwig et al., 2016; Spötl et al., 2021; Velasquez et al., 2022; Del Gobbo et al., 2023; Russo et al., 2024) and governed the distribution of ELAs across the mountain range (Kuhlemann et al., 2008; Hughes and Woodward, 2016; Višnjević et al., 2020; Del Gobbo et al., 2023). These climatic data also supported palaeoglaciological models and contributed to their improvement (Seguinot et al., 2018; Jouvet et al., 2023; Leger et al., 2025). The availability of empirical ELA reconstructions aids model–data comparisons and gives new hints for model validation and better resolution. In the south-eastern Alps many LGM glaciers located in isolated mountains have been reconstructed over the last few years (Baratto et al., 2003; Monegato, 2012; Rettig et al., 2021, 2023) and have provided important information on LGM temperature and precipitation rates along the Alpine fringe. Nevertheless, the climatic conditions in more internal parts of the Alps have remained poorly constrained because of the difficulties in estimating the ELAs for large valley glacier networks (Pellitero et al., 2016). The new data provided in the present work help to solve this gridlock. The lateral moraines, which normally start to form at the transition from accumulation to ablation areas (Lichtenecker, 1938), appear just above 1500 m a.s.l. in the western, upper reach of the Valsugana area. This is in agreement with the ELA of the largest isolated glacier of the area, that of Monte Coppolo. The calculated ELAs also show good agreement with the modelled ELA from Del Gobbo et al. (2023), in which the 1500 m a.s.l. ELA contour crosses the Valsugana Valley, while for both the Cima d'Asta and the Sette Comuni Plateau, higher ELA values were modelled.

However, while an ELA of ca. 1500 m a.s.l. can be considered an average for the glacier system, differences between ELAs of smaller ice masses point to variations within both local topoclimate and regional precipitation patterns, as shown by N–S cross sections from the Venetian–Friulian Plain to the Cima d'Asta sector (Fig. 8). These cross sections show an ELA rise of about 200–300 m within the first few kilometres of the Alpine fringe, which is independent of glacier aspect. Assuming non-significant temperature gradients over these short distances, the ELA gradient most likely reflects changes in the precipitation rate moving from the Alpine fringe towards the more interior parts of the mountain range. Applying an LGM summer temperature depression of ca. 10 °C (Samartin et al., 2016; Pini et al., 2022) and using the P/T relationship by Ohmura and Boettcher (2018), calculated palaeoprecipitation would be around 1800 mm yr^{-1} in the first prealpine chain facing the Venetian–Friulian Plain (e.g. at Monte Grappa) and decrease to just over 1400 mm yr^{-1} towards the Cima d'Asta massif – a fall in the precipitation rate of about 400 mm yr^{-1} over just 30–40 km of horizontal distance (see Fig. 8). Similar trends in reconstructed palaeoprecipitation have also been observed in other formerly glaciated mountain ranges in Europe, such as in the Balkan Peninsula (Ruszkiczay-Rüdiger et al., 2022). This trend of increase in aridity towards the inner sector could also explain why, despite the higher catchment elevation of the Cima d'Asta massif, the Valsugana trunk glacier flowed into the Malene Valley. This casts new light on the relationships between trunk glaciers and their tributaries under the influence of local and regional climatic gradients in complex mountainous topographies.

6 Conclusions

In this study, we present new insights into the evolution of Last Glacial Maximum (LGM) glaciers in the Valsugana, south-eastern European Alps. We combine geomorphological mapping with ^{10}Be surface exposure dating and reconstructions of palaeoglacier equilibrium line altitudes (ELAs) to strengthen the chronology of ice advances in the area and

to better understand their climatic controls. The following points can be concluded from our data:

1. During the LGM, the Valsugana (upper Brenta catchment) was covered by an interconnected glacier network. The reconstruction of this glacier network could be refined through detailed geomorphological mapping of ice-marginal features such as lateral moraine ridges and trimlines.

2. Within the LGM glacier network, several isolated mounts remained free of ice, such as the Monte Lefre nunatak, where lateral moraines are preserved at elevations up to 1360 m a.s.l. ^{10}Be surface exposure ages from erratic boulders at Monte Lefre suggest that the moraines were formed between 20 and 19 ka. This demonstrates that the Valsugana glacier remained at an elevated position until the very end of the global LGM and that ice surface lowering in the area was not initiated before 19 ka.

3. Separated from the glacier network, smaller isolated glaciers existed during the LGM. The reconstructed ELAs of these marginal ice masses lie between 1500 and 1700 m a.s.l. Different ELAs can be explained by (1) catchment aspect and (2) climatic gradient, with lowering precipitation from the foreland plain and Prealps to the inner-alpine sector.

4. The N–S gradient of decreasing ELAs suggests a decrease in precipitation of Mediterranean humid air masses moving from the foreland of the Alps towards the more internal sectors of the mountain range. Local climatic gradients such as this one found in the Valsugana may have been important for the evolution of LGM glaciers elsewhere and need to be accounted for in glacier and palaeoclimate modelling approaches.

Data availability. Data related to the geological mapping are available from ISPRA on a dedicated website (https://progetto-carg.isprambiente.it/cartografiaCARG/index.php?source=cartageologica&regione=Trentino-Alto+Adige&foglio=061, last access: 1 October 2025). All other data (e.g. glacier reconstructions, exposure age data) will be made available upon request to the authors.

Author contributions. LR, SR, and GM undertook major roles in the conceptualization, project organization, preparation of the manuscript, and artwork. LR, SK, SIO, and MC worked on cosmogenic nuclide dating and interpretation. EM and SM contributed with fieldwork data collection. All the authors were involved in the final draft of the manuscript.

Competing interests. The contact author has declared that none of the authors has any competing interests.

Disclaimer. Publisher's note: Copernicus Publications remains neutral with regard to jurisdictional claims made in the text, published maps, institutional affiliations, or any other geographical representation in this paper. While Copernicus Publications makes every effort to include appropriate place names, the final responsibility lies with the authors.

Acknowledgements. The authors are grateful to the editor Zsófia Ruszkiczay-Rüdiger and to Felix Martin Hofmann and Jerzy Zasadni for their revisions, which highly improved the manuscript.

Financial support. This work was carried out in the frame of the CARG project (sheet 061 Borgo Valsugana). Funding for AMS measurements was provided through RADIATE Transnational Access (proposal number 22002973), while Sarah Kamleitner was funded by the Swiss National Science Foundation (SNSF grant number 175794, 2017) for the duration of the project.

Review statement. This paper was edited by Zsófia Ruszkiczay-Rüdiger and reviewed by Jerzy Zasadni and Felix Martin Hofmann.

References

Akçar, N., Ivy-Ochs, S., Kubik, P. W., and Schlüchter, C.: Post-depositional impacts on 'Findlinge' (erratic boulders) and their implications for surface-exposure dating, Swiss J. Geosci., 104, 445–453, https://doi.org/10.1007/s00015-011-0088-7, 2011.

André, M. F.: Rates of postglacial rock weathering on glacially scoured outcrops (Abisko–Riksgränsen area, 68?n), Geogr. Ann. Phys. Geogr., 84, 139–150, https://doi.org/10.1111/j.0435-3676.2002.00168.x, 2002.

Antonelli, R., Barbieri, G., Dal Pra, A., De Zanche, V., Grandesso, P., Mietto, P., Sedea, R., and Zanferrari, A.: Carta Geologica del Veneto – una storia di cinquecento milioni di anni, 1 carta geol., SELCA, Firenze, 32 pp., 1990.

Auer, I., Böhm, R., Jurkovic, A., Lipa, W., Orlik, A., Potzmann, R., Schöner, W., Ungersböck, M., Matulla, C., Briffa, K., Jones, P., Efthymiadis, D., Brunetti, M., Nanni, T., Maugeri, M., Mercalli, L., Mestre, O., Moisselin, J.-M., Begert, M., Müller-Westermeier, G., Kveton, V., Bochnicek, O., Stastny, P., Lapin, M., Szalai, S., Szentimrey, T., Cegnar, T., Dolinar, M., Gajic-Capka, M., Zaninovic, K., Majstorovic, Z., and Nieplova, E.: HISTALP – historical instrumental climatological surface time series of the Greater Alpine Region, Int. J. Climatol., 27, 17–46, https://doi.org/10.1002/joc.1377, 2007.

Avanzini, M., Bargossi, G. M., Borsato, A., and Selli, L.: Note Illustrative della Carta Geologica d'Italia alla scala 1: 50.000, foglio 060-Trento, ISPRA-Servizio Geologico d'Italia, Trento, 2010.

Balco, G., Stone, J. O., Lifton, N. A., and Dunai, T. J.: A complete and easily accessible means of calculating surface exposure ages or erosion rates from ^{10}Be and ^{26}Al measurements, Quat. Geochronol., 3, 174–195, https://doi.org/10.1016/j.quageo.2007.12.001, 2008.

Balco, G., Briner, J., Finkel, R. C., Rayburn, J. A., Ridge, J. C., and Schaefer, J. M.: Regional beryllium-

10 production rate calibration for late-glacial northeastern North America, Quat. Geochronol., 4, 93–107, https://doi.org/10.1016/j.quageo.2008.09.001, 2009.

Baratto, A., Ferrarese, F., Meneghel, M., and Sauro, U.: La ricostruzione della glaciazione Wurmiana nel Gruppo del Monte Grappa (Prealpi Venete), in: Risposta dei processi geomorfologici alle variazioni ambientali, edited by: Biancotti, A. and Motta, M., Brigati G., Genova, 67–77, 2003.

Barbieri, G. and Grandesso, P.: Note illustrative della Carta Geologica d'Italia alla scala 1: 50.000, foglio 082-Asiago, APAT, S.EL.CA., Firenze, 135, 2007.

Benn, D. I. and Hulton, N. R. J.: An ExcelTM spreadsheet program for reconstructing the surface profile of former mountain glaciers and ice caps, Comput. Geosci., 36, 605–610, https://doi.org/10.1016/j.cageo.2009.09.016, 2010.

Bini, A., Buoncristiani, J. F., Couterrand, S., Ellwanger, D., Felber, M., Florineth, D., Graf, H. R., Keller, O., Kelly, M., Schlüchter, C., and Schöneich, P.: Die Schweiz während des letzteiszeitlichen Maximums (LGM), Bundesamt für Landestopographie swisstopo, Wabern, 2009.

Bondesan, A., Calderoni, G., and Mozzi, P.: L'assetto geomorfologico della pianura veneta centro-orientale: stato delle conoscenze e nuovi dati, in: Scritti in ricordo di Giovanna Brunetta, edited by: Varotto, M. and Zunica, M., Università degli Studi di Padova, Dipartimento di Geografia, Padova, 19–38, 2002.

Braakhekke, J., Ivy-Ochs, S., Monegato, G., Gianotti, F., Martin, S., Casale, S. and Christl, M.: Timing and flow pattern of the Orta glacier (European Alps) during the last glacial maximum. Boreas, 49, 315–332, https://doi.org/10.1111/bor.12427, 2020.

Burke, R. M. and Birkeland, P. W.: Reevaluation of multiparameter relative dating techniques and their application to glacial sequences along the eastern Sierra Nevada, California, Quaternary Res., 2, 21–51, 1979.

Carraro, F. and Sauro, U.: Il Glacialismo "locale" Wurmiano del Massiccio del Grappa (Provincie di Treviso e di Vicenza), Geogr. Fis. Din. Quat., 2, 6–16, 1979.

Carton, A., Bondesan, A., Fontana, A., Meneghel, M., Miola, A., Mozzi, P., Primon, S., and Surian, N.: Geomorphological evolution and sediment transfer in the Piave River system (northeastern Italy) since the Last Glacial Maximum, Géomorphologie, 15, 155–174, https://doi.org/10.4000/geomorphologie.7639, 2009.

Castiglioni, B.: L'Italia nell'età quaternaria, Atlante Fisicoeconomico d'Italia, Consociazione Turistica Italiana, Milano, Italy, 1940.

Chaline, J. and Jerz, H.: Arbeitsergebnisse der Subkommission für Europäische Quartärstratigraphie. Stratotypen des Würm-Glazials, Eiszeitalter und Gegenwart, 35, 185–206, 1984.

Chandler, B. M., Lovell, H., Boston, C. M., Lukas, S., Barr, I. D., Benediktsson, Í.Ö., Benn, D. I., Clark, C. D., Darvill, C .M., Evans, D. J., Ewertowski, M. W., Loibl, D., Margold, M., Otto, J.-C., Roberts, D. H., Stokes, C. R., Storrar, R. D., and Stroeven, A. P.: Glacial geomorphological mapping: A review of approaches and frameworks for best practice, Earth-Sci. Rev., 185, 806–846, https://doi.org/10.1016/j.earscirev.2018.07.015, 2018.

Clark, P. U., Dyke, A. S., Shakun, J. D., Carlson, A. E., Clark, J., Wohlfarth, B., Mitrovica, J. X., Hostetler, S. W., and McCabe, A. M.: The last glacial maximum, Science, 325, 710–714, https://doi.org/10.1126/science.1172873, 2009.

Claude, A., Ivy-Ochs, S., Kober, F., Antognini, M., Salcher, B., and Kubik, P. W.: The Chironico landslide (Valle Leventina, southern Swiss Alps): age and evolution, Swiss J. Geosci., 107, 273–291, https://doi.org/10.1007/s00015-014-0170-z, 2014.

Coleman, C. G., Carr, S. J., and Parker, A. G.: Modelling topoclimatic controls on palaeoglaciers: implications for inferring palaeoclimate from geomorphic evidence, Quaternary Sci. Rev., 28, 249–259, https://doi.org/10.1016/j.quascirev.2008.10.016, 2009.

Colman, S. and Pierce, K.: Glacial Sequence Near McCall, Idaho: Weathering Rinds, Soil Development, Morphology, and Other Relative-Age Criteria, Quaternary Res., 25, 25–42, https://doi.org/10.1016/0033-5894(86)90041-4, 1986.

Coutterand, S., Schoeneich, P., and Nicoud, G.: Le lobe glaciaire lyonnais au maximum würmien: glacier du Rhône ou/et glaciers savoyard? Neige et glace de montagne, reconstitution, dynamique, pratiques, Collection EDYTEM, Cahiers de Gèographie, 8, 11–22, 2009.

Cucato, M.: Rilevamento della media Val d'Astico (Provincia di Vicenza): saggio per l'applicazione della normativa sulla cartografia geologica del Quaternario continentale, Bollettino Servizio Geologico D'Italia, 115, 99–130, 2001.

Cucato, M.: La successione continentale Pliocenico(?) - quaternaria, in: Note Illustrative della Carta geologica d'Italia alla scala 1:50000, edited by: Barbieri, G. and Grandesso, P., Foglio 082 "Asiago", APAT – Dip. Difesa del Suolo – Servizio Geologico d'Italia – Regione del Veneto, S.EL.CA. s.r.l., Firenze, 60–94, 2007.

Del Gobbo, C., Colucci, R. R., Monegato, G., Žebre, M., and Giorgi, F.: Atmosphere–cryosphere interactions during the last phase of the Last Glacial Maximum (21 ka) in the European Alps, Clim. Past, 19, 1805–1823, https://doi.org/10.5194/cp-19-1805-2023, 2023.

Ehlers, J. and Gibbard, P. L.: Quaternary Glaciations Extent and Chronology, Part I: Europe, Elsevier, Amsterdam, https://doi.org/10.1002/jqs.1050, 2004.

Ehlers, J., Gibbard, P. L., and Hughes, P. D. (Eds.): Quaternary Glaciations – Extent and Chronology, A Closer Look, Elsevier Science, London, ISBN 9780444534477, 2011.

Evans, D. and Benn, D.: A Practical Guide to the Study of Glacial Sediments, Quaternary Research Association, ISBN 0-340-75959-3, 2021.

Felber, M., Veronese, L., Cocco, S., Frei, W., Nardin, M., Oppizzi, P., Santuliana, E., and Violanti, D.: Indagini sismiche e geognostiche nelle valli del Trentino meridionale (Val d'Adige, Valsugana, Valle del Sarca, Valle del Chiese), St. Trent. Sc. Nat., Acta Geol., 75, 3–52, 1998.

Furbish, D. J. and Andrews, J. T.: The use of hypsometry to indicate long-term stability and response of valley glaciers to changes in mass transfer, J. Glaciol., 30, 199–211, https://doi.org/10.3189/S0022143000005931, 1984.

Galadini, F., Poli, M. E., and Zanferrari, A.: Seismogenic sources potentially responsible for earthquakes with M≥6 in the eastern Southern Alps (Thiene-Udine sector, NE Italy), Geophys. J. Int., 161, 739–762, https://doi.org/10.1111/j.1365-246X.2005.02571.x, 2005.

Gosse, J. C. and Phillips, F. M.: Terrestrial in situ cosmogenic nuclides: theory and applications, Quaternary Sci. Rev., 20, 1475–1560, https://doi.org/10.1016/S0277-3791(00)00171-2, 2001.

Hofmann, F. M., Steiner, M., Hergarten, S., ASTER Team, and Preusser, F.: Limitations of precipitation reconstructions using equilibrium-line altitudes exemplified for former glaciers in the Southern Black Forest, Central Europe., Quaternary Res., 117, 135–159, https://doi.org/10.1017/qua.2023.53, 2024.

Hughes, P. and Woodward J.: Quaternary glaciation in the Mediterranean mountains: a new synthesis, Geological Society, London, Special Publications, 433, https://doi.org/10.1144/sp433.14, 2016.

Ivy-Ochs, S.: The Dating of Rock Surfaces Using in Situ Produced ^{10}Be, ^{26}Al and ^{36}Cl, with Examples from Antarctica and the Swiss Alps, ETH Zürich, PhD dissertation, 210 pp., https://doi.org/10.3929/ethz-a-001772745, 1996.

Ivy-Ochs, S. and Kober, F.: Surface exposure dating with cosmogenic nuclides, E&G Quaternary Sci. J., 57, 179–209, https://doi.org/10.3285/eg.57.1-2.7, 2008.

Ivy-Ochs, S., Lucchesi, S., Baggio, P., Fioraso, G., Gianotti, F., Monegato, G., Graf, A. A., Akçar, N., Christl, M., Carraro, F., Forno, M. G., and Schlüchter, C.: New geomorphological and chronological constraints for glacial deposits in the Rivoli-Avigliana end-moraine system and the lower Susa Valley (Western Alps, NW Italy), J. Quaternary Sci., 33, 550–562, https://doi.org/10.1002/jqs.3034, 2018.

Ivy-Ochs, S., Monegato, G., and Reitner, J. M.: The Alps: glacial landforms from the last glacial maximum, in: European Glacial Landscapes: Maximum Extent of Glaciations, edited by: Palacios, D., Hughes, P. D., García-Ruiz, J. M., and Andrés, N., Elsevier, Amsterdam, 449–460, https://doi.org/10.1016/B978-0-12-823498-3.00030-3, 2022.

Jäckli, H., Hantke, R., Imhof, E., and Leuzinger, H.: Die Schweiz zur letzten Eiszeit = La Suisse durant la dernière période glaciaire = La Svizzera durante l'ultima glaciazione, Atlas der Schweiz 6, Eidg. Landestopographie, Wabern, 1973.

Jouvet, G., Cohen, D., Russo, E., Buza, J., Raible, C. C., Haeberli, W., Kamleitner, S., Ivy-Ochs, S., Imhof, M. A., Becker, J. K., Landgraf, A., and Fischer U. H.: Coupled climate-glacier modelling of the last glaciation in the Alps, J. Glaciol., 69, 1956–1970, https://doi.org/10.1017/jog.2023.74, 2023.

Kamleitner, S., Ivy-Ochs, S., Monegato, G., Gianotti, F., Akçar, N., Vockenhuber, C., Christl, M., and Synal, H. A.: The Ticino-Toce glacier system (Swiss-Italian Alps) in the framework of the alpine last glacial maximum, Quaternary Sci. Rev., 279, 107400, https://doi.org/10.1016/j.quascirev.2022.107400, 2022.

Kamleitner, S., Ivy-Ochs, S., Manatschal, L., Akçar, N., Christl, M., Vockenhuber, C., Hajdas, I., and Synal, H. A.: Last Glacial Maximum glacier fluctuations on the northern Alpine foreland: geomorphological and chronological reconstructions from the Rhine and Reuss glacier systems, Geomorphology, 423, 108548, https://doi.org/10.1016/j.geomorph.2022.108548, 2023.

Kohl, C. P. and Nishiizumi, K.: Chemical isolation of quartz for measurement of in-situ produced cosmogenic nuclides, Geochem. Cosmochim. Ac., 56, 3583–3587, https://doi.org/10.1016/0016-7037(92)90401-4, 1992.

Kronig, O., Ivy-Ochs, S., Hajdas, I., Christl, M., Wirsig, C., and Schlüchter, C.: Holocene evolution of the Triftje- and the Oberseegletscher (Swiss Alps) constrained with 10Be exposure and radiocarbon dating, Swiss J. Geosci., 111, 117–131, https://doi.org/10.1007/s00015-017-0288-x, 2018.

Kuhlemann, J., Rohling, E. J., Krumrei, I., Kubik, P., Ivy-Ochs, S., and Kucera, M.: Regional synthesis of mediterranean atmospheric circulation during the last glacial maximum, Science, 321, 1338–1340, https://doi.org/10.1126/science.1157638, 2008.

Lal, D.: Cosmic ray labeling of erosion surfaces: in situ nuclide production rates and erosion models, Earth Planet. Sc. Lett., 104, 424–439, https://doi.org/10.1016/0012-821X(91)90220-C, 1991.

Leger, T. P. M., Jouvet, G., Kamleitner, S. Mey, J., Herman, F., Finley, B. D., Ivy-Ochs, S., Vieli A., Hnez, A., and Nussbaumer, S. U.: A data-consistent model of the last glaciation in the Alps achieved with physics-driven AI, Nat. Commun., 16, 848, https://doi.org/10.1038/s41467-025-56168-3, 2025.

Li, Y.: PalaeoIce: An automated method to reconstruct palaeoglaciers using geomorphic evidence and digital elevation models, Geomorphology, 421, 108523, https://doi.org/10.1016/j.geomorph.2022.108523, 2023.

Lichtenecker, N.: Die gegenwârtige und die eiszeitliche Schneegrenze in den Ostalpen, in: Verhandlungen der III Internationalen Quartär -Konferenz, edited by: Gôtzinger, G., Vienna, September 1936, 141–147, INQUA, Vienna, Austria, 1938.

Ludwig, P., Schaffernicht, E. J., Shao, Y., and Pinto, J. G.: Regional atmospheric circulation over Europe during the Last Glacial Maximum and its links to precipitation, J. Geophys. Res., 121, 2130–2145, https://doi.org/10.1002/2015JD024444, 2016.

Lukas, S.: Morphostratigraphic principles in glacier reconstruction-a perspective from the British Younger Dryas, Prog. Phys. Geogr., 30, 719–736, https://doi.org/10.1177/0309133306071955, 2016.

Maxeiner, S., Synal, H. A., Christl, M., Suter, M., Müller, A., and Vockenhuber, C.: Proof-of-principle of a compact 300 kV multi-isotope AMS facility, Nucl. Instrum. Meth. B, 439, 84–89, https://doi.org/10.1016/j.nimb.2018.11.028, 2019.

Monegato, G.: Local glaciers in the Julian Prealps (NE Italy) during the Last Glacial Maximum, Alpine and Mediterranean Quaternary, 25, 5–14, 2012.

Monegato, G., Ravazzi, C., Donegana, M., Pini, R., Calderoni, G., and Wick, L.: Evidence of a two-fold glacial advance during the last glacial maximum in the Tagliamento end moraine system (eastern Alps), Quaternary Res., 68, 284–302, https://doi.org/10.1016/j.yqres.2007.07.002, 2007.

Monegato, G., Scardia, G., Hajdas, I., Rizzini, F., and Piccin, A.: The Alpine LGM in the boreal ice-sheets game, Sci. Rep., 7, 2078, https://doi.org/10.1038/s41598-017-02148-7, 2017.

Nye, J. F.: A method of calculating the thicknesses of the ice-sheets, Nature, 169, 529–530, https://doi.org/10.1038/169529a0, 1952.

Nye, J. F.: The flow of a Glacier in a channel of rectangular, elliptic or parabolic cross-section, J. Glaciol., 5, 661–690, https://doi.org/10.3189/S0022143000018670, 1965.

Ohmura, A. and Boettcher, M.: Climate on the equilibrium line altitudes of glaciers: theoretical background behind Ahlmann's P/T diagram, J. Glaciol., 64, 489–505, https://doi.org/10.1017/jog.2018.41, 2018.

Oien, R. P., Rea, B. R., Spagnolo, M., Barr, I. D., and Bingham, R. G.: Testing the area-altitude balance ratio (AABR) and accumulation-area ratio (AAR) methods of calculating glacier equilibrium-line altitudes, J. Glaciol., 68, 357–368, https://doi.org/10.1017/jog.2021.100, 2022.

Pellitero, R., Rea, B. R., Spagnolo, M., Bakke, J., Hughes, P., Ivy-Ochs, S., Lukas, S., and Ribolini, A.: A GIS tool for automatic calculation of glacier equilibrium-line altitudes, Comput. Geosci., 82, 55–62, https://doi.org/10.1016/j.cageo.2015.05.005, 2015.

Pellitero, R., Rea, B. R., Spagnolo, M., Bakke, J., Ivy-Ochs, S., Frew, C. R., Hughes, P., Ribolini, A., Lukas, S., and Renssen, H.: GlaRe, a GIS tool to reconstruct the 3D surface of palaeoglaciers, Comput. Geosci., 94, 77–85, https://doi.org/10.1016/j.cageo.2016.06.008, 2016.

Penck, A.: Die Vergletscherung der Deutschen Alpen, ihre Ursachen, periodische Wiederkehr und ihr Einfluss auf die Bodengestaltung, Johann Ambrosius Barth, Leipzig, 483 pp., 1882.

Penck, A. and Brückner, E.: Die Alpen im Eiszeitalter, Tauchnitz, Leipzig, 1901–1909.

Pezzotta, A., Mariani, G. S., Marini, M., Cremaschi, M., and Zerboni, A.: Last Glacial Maximum glaciolacustrine deposits from the Adige Moraine Amphitheatre (Rivoli Veronese, Northern Italy): distribution, sedimentary facies, and significance, Alpine and Mediterranean Quaternary, 37, 29–51, https://doi.org/10.26382/AMQ.2024.02, 2024.

Pini, R., Furlanetto, G., Vallé, F., Badino, F., Wick, L., Anselmetti, F .S., Bertuletti, P., Fusi, N., Morlock, M. A., Delmonte, B., Harrison, S. P., Maggi, V., and Ravazzi, C.: Linking North Atlantic and Alpine Last Glacial Maximum climates via a high-resolution pollen-based subarctic forest steppe record, Quaternary Sci. Rev., 294, 107759, https://doi.org/10.1016/j.quascirev.2022.107759, 2022.

Poli, M. E., Patricelli, G., Monegato, G., and Zanferrari, A.: Structural inheritances, fault segmentation and seismogenic potential at the front of the eastern Southern Alps (central Carnic Prealps, NE Italy), Tectonophysics, 883, 230390, https://doi.org/10.1016/j.tecto.2024.230390, 2024.

Rea, B. R.: Defining modern day Area-Altitude Balance Ratios (AABRs) and their use in glacier-climate reconstructions, Quaternary Sci. Rev., 28, 237–248, https://doi.org/10.1016/j.quascirev.2008.10.011, 2009.

Rettig, L., Monegato, G., Mozzi, P., Žebre, M., Casetta, L., Fernetti, M., and Colucci, R. R.: The Pleistocene evolution and reconstruction of LGM and late glacial paleoglaciers of the Silisia Valley and Mount Raut (Carnic Prealps, NE Italy), Alpine and Mediterranean Quaternary, 34, 277–290, https://doi.org/10.26382/AMQ.2021.17, 2021.

Rettig, L., Monegato, G., Spagnolo, M., Hajdas, I., and Mozzi, P.: The Equilibrium Line Altitude of isolated glaciers during the Last Glacial Maximum – New insights from the geomorphological record of the Monte Cavallo Group (south-eastern European Alps), Catena, 229, 107187, https://doi.org/10.1016/j.catena.2023.107187, 2023.

Roattino, T., Crouzet, C., Vassallo, R., Buoncristiani, J.-F., Carcaillet, J., Gribenski, N., and Valla, P. G.: Paleogeographical reconstruction of the western French Alps foreland during the last glacial maximum using cosmogenic exposure dating, Quaternary Res., 111, 68–83, https://doi.org/10.1017/qua.2022.25, 2023.

Rodés, Á.: Cosmogenic Exposure Age Averages, github.com/angelrodes/CEAA, Zenodo, https://doi.org/10.5281/zenodo.4024909, 2020.

Roghi, G., Monegato, G., Zambotti, P., De Mozzi, M., Rinaldo, M., Trentini, T., Montresor, L., Modesti, A., Gosio, F., Bartoli, O., Piccin, G., Favaro, S., and Martin S.: Sedimentary evolution of Valsugana area in the geologic record of 61 "Borgo Valsugana" Sheet, SGI Meeting: The Geoscience paradigm: Resources, Risks and future perspectives, Potenza, 19–21 September 2023, 2023.

Rossato, S. and Mozzi, P.: Inferring LGM sedimentary and climatic changes in the southern Eastern Alps foreland through the analysis of a ^{14}C ages database (Brenta megafan, Italy), Quaternary Sci. Rev., 148, 115–127, https://doi.org/10.1016/j.quascirev.2016.07.013, 2016.

Rossato, S., Monegato, G., Mozzi, P., Cucato, M., Gaudioso, B., and Miola, A.: Late Quaternary glaciations and connections to the piedmont plain in the prealpine environment: the middle and lower Astico Valley (NE Italy), Quaternary Int., 288, 8–24, https://doi.org/10.1016/j.quaint.2012.03.005, 2013.

Rossato, S., Carraro, A., Monegato, G., Mozzi, P., and Tateo, F.: Glacial dynamics in pre-Alpine narrow valleys during the Last Glacial Maximum inferred by lowland fluvial records (northeast Italy), Earth Surf. Dynam., 6, 809–828, https://doi.org/10.5194/esurf-6-809-2018, 2018.

Russo, E., Buzan, J., Lienert, S., Jouvet, G., Velasquez Alvarez, P., Davis, B., Ludwig, P., Joos, F., and Raible, C. C.: High-resolution LGM climate of Europe and the Alpine region using the regional climate model WRF, Clim. Past, 20, 449–465, https://doi.org/10.5194/cp-20-449-2024, 2024.

Ruszkiczay-Rüdiger, Z., Temovski, M., Kern, Z., Madarász, B., Milevski, I., Lachner, J., and Steier, P.: Late Pleistocene glacial advances, equilibrium-line altitude changes and paleoclimate in the Jakupica Mts (North Macedonia), Catena, 216, 106383, https://doi.org/10.1016/j.catena.2022.106383, 2022.

Samartin, S., Heiri, O., Kaltenrieder, P., Kuehl, N., and Tinner, W.: Reconstruction of full glacial environments and summer temperatures from Lago della Costa, a refugial site in Northern Italy, Quaternary Sci. Rev., 143, 107–119, https://doi.org/10.1016/j.quascirev.2016.04.005, 2016.

Schilling, D. H. and Hollin, J. T.: Numerical reconstructions of valley glaciers and small ice caps, in: The Last Great Ice Sheets, edited by: Denton, G. H. and Hughes, T. J., Wiley, New York, 207–220, 1981.

Seguinot, J., Ivy-Ochs, S., Jouvet, G., Huss, M., Funk, M., and Preusser, F.: Modelling last glacial cycle ice dynamics in the Alps, The Cryosphere, 12, 3265–3285, https://doi.org/10.5194/tc-12-3265-2018, 2018.

Smith, M. J., Rose, J., and Booth, S.: Geomorphological mapping of glacial landforms from remotely sensed data: an evaluation of the principal data sources and an assessment of their quality, Geomorphology, 76, 148–165, https://doi.org/10.1016/j.geomorph.2005.11.001, 2006.

Spötl, C., Koltai, G., Jarosch, A. H., and Cheng, H.: Increased autumn and winter precipitation during the Last Glacial Maximum in the European Alps, Nat. Commun., 12, 1839, https://doi.org/10.1038/s41467-021-22090-7, 2021.

Stone, J. O.: Air pressure and cosmogenic isotope production, J. Geophys. Res.-Sol. Ea., 105, 23753–23759, https://doi.org/10.1029/2000JB900181, 2000.

Tarquini, S., Isola, I., Favalli, M., Mazzzarini, F., Bisson, M., Pareschi, M.T., and Boschi, E.: TINITALY/01: a new Triangular Irregular Network of Italy, Ann. Geophys., 50, 407–425, https://doi.org/10.4401/ag-4424, 2007.

Tarquini, S., Isola, I., Favalli, M., Battistini, A., and Dotta, G.: TINITALY, a digital elevation model of Italy with a 10 meters cell size (Version 1.1), Istituto Nazionale di Geofisica e Vulcanologia (INGV), https://doi.org/10.13127/tinitaly/1.1, 2023.

Tomkins, M. D., Dortch, J. M., Hughes, P. D., Huck, J. J., Pallàs, R., Rodés, Á., Allard, J. L., Stimson, A. G., Bourlès, D., Rinterknecht, V., Jomelli, V., Rodríguez-Rodríguez, L., Copons, R., Barr, I. D., Darvill, C. M., and Bishop, T: Moraine crest or slope: An analysis of the effects of boulder position on cosmogenic exposure age, Earth Planet. Sc. Lett., 570, 117092, https://doi.org/10.1016/j.epsl.2021.117092, 2021.

van Husen, D.: Die Ostalpen in den Eiszeiten, Veröffentlichungen der Geologischen Bundesanst, 2, 1–24, 1987.

Valt, M., Cianfarra, P., and Valt., M.: Neve e clima sulle Alpi Italiane, Neve e Valanghe, 96, 1–15, 2022.

Velasquez, P., Messmer, M., and Raible, C. C.: The role of ice-sheet topography in the Alpine hydro-climate at glacial times, Clim. Past, 18, 1579–1600, https://doi.org/10.5194/cp-18-1579-2022, 2022.

Venzo, S.: I depositi quaternari e del neogene superiore nella bassa valle del Piave da Quero al Montello e del Paleopiave nella valle del Soligo (Treviso), Memorie degli Istituti di Geologia e Mineralogia dell'Università di Padova, 30, 1–64, 1977.

Višnjević, V., Herman, F., and Prasicek, G.: Climatic patterns over the European Alps during the LGM derived from inversion of the paleo-ice extent, Earth Planet. Sc. Lett., 538, 116185, https://doi.org/10.1016/j.epsl.2020.116185, 2020.

Wirsig, C., Zasadni, J., Christl, M., Akçar, N., and Ivy-Ochs, S.: Dating the onset of LGM ice surface lowering in the High Alps, Quaternary Sci. Rev., 143, 37–50, https://doi.org/10.1016/j.quascirev.2016.05.001, 2016.